

MODELING AND CONTROL OF KARMAN VORTEX STREETS

E. Roesch⁺, F. Ohle^{+*}, H. Eckelmann⁺, A. Hübler^{*}

⁺ Institut für Angewandte Mechanik und Strömungsphysik
der Universität Göttingen,
D-3400 Göttingen, F.R.G.

^{*} Department of Physics, University of Illinois and Beckmann Institute,
Center of Complex Systems Research, Urbana-Champaign, IL 61801, USA

1. INTRODUCTION

One of the most important problems in hydrodynamics is the behaviour of low-dimensional dynamics in closed and open flows. Lorenz¹ and Ruelle & Takens² proposed that the dynamics of a hydrodynamic system at the onset of turbulence could be described by strange attractors and low-dimensional differential equations. This was in contrast to Landau's³ hypothesis that turbulence is a quasiperiodic phenomenon with an infinite number of frequencies.

Brandstätter et al.⁴ could experimentally verify low-dimensional dynamics with Lyapunov exponents and generalized dimensions in a closed hydrodynamic flow, namely in Taylor-Couette flow, and could thus disprove the hypothesis of Landau. The first work dealing with chaotic dynamics in an open hydrodynamic system stems from Olinger & Sreenivasan⁵. From the partly chaotic behaviour of a sinusoidally driven Kármán vortex street in this work it can be inferred that the original dynamics of a vortex street might be described by a van der Pol oscillator. This was postulated by Benaroya & Lepore⁶. Investigating experimentally mode-locking states of Kármán vortex streets Detemple⁷ concluded from the response that a van der Pol oscillator might be an appropriate model for the dynamics of the vortex street. Nevertheless, there are essential differences between the response of a van der Pol oscillator and of the vortex street.

In this investigation differential equations are extracted from experimental time series obtained in Kármán vortex streets. It will be shown that the velocity signal measured in the regular range of a vortex street ($50 \leq Re \leq 150$) can be modeled by a second order differential equation with ten parameters. The parameters are nearly independent of the probe position and of the Reynolds number. With the knowledge of the constructed differential equation the response of the vortex street on perturbations can be predicted.

2. CONSTRUCTION OF DIFFERENTIAL EQUATIONS

The complete construction of a differential equation is based on a fit of the flow vector field by series of orthogonal polynomials. For most of the non-linear oscillators investigated so far, the flow vector fields can be described by Taylor expansions with a small number of non-vanishing coefficients. The parameters obtained by the fit are an approximation of the coefficients of the underlying differential equation. These parameters can be determined from an experimental set of data given as a time series. In a first step, these time series are numerically differentiated, thus providing the state space representation necessary to determine the complete flow vector field F as a function of the state space vector (x_1, x_2) . The number of components of the flow vector field, and thus also the order of the differential equation, increase in proportion to the dimension of the state space representation. In the next step each component of the flow vector field is approximated separately by a series of Legendre polynomials up to the order p :

$$F_1(x_1, x_2) = \sum_{i,j=0}^{i+j \leq p} a_{ij} L_i(x_1) L_j(x_2);$$

$$F_2(x_1, x_2) = \sum_{i,j=0}^{i+j \leq p} b_{ij} L_i(x_1) L_j(x_2).$$

Because of their orthogonality Legendre polynomials are appropriate for the approximation used here. The magnitude of the fit coefficients is nearly independent of the order p of the approximation which is based here on a general linear least square fit. Since the orthogonality of the Legendre polynomials is only valid for $|x| \leq 1$, all values have to be normalized to this range. The quality of a fit is estimated by the quantity χ which is defined by the equation:

$$\chi^2 = \sum_i \frac{|\underline{f}_j^i - \underline{f}_j(\underline{r}_i)|^2}{|\Delta \underline{f}_j^i|^2}.$$

Here \underline{f}_j^i is the experimental value of the component j at the position \underline{r}_i , $\underline{f}_j(\underline{r}_i)$ is the adapted value and $\Delta \underline{f}_j^i$ is the error of the respective experimental data. The theoretical value of χ is the number of the data minus the number of parameters of the fit. The order of the fit is successively raised until χ has approximately reached the theoretical value.

It is only possible to approximate a flow vector field in the surrounding of the attractor if the flow vectors have been derived from this region of the state space. A fit is best, when the positions of the calculated flow vectors are homogeniously distributed in the region of interest. Therefore, it is also necessary to investigate the transient states if a system has a fixed point or a limit cycle as an attractor. In the case of a chaotic dynamic the fit is especially good since chaotic trajectories fill the state space quite regularly.

The quality of a fit is checked by a numerical integration of the constructed differential equation. In a state space representation the global geometry of the trajectories of the numerical and the experimental data are directly compared.

3. EXPERIMENTAL SETUP

The measurements were carried out in the open-return wind tunnel described by Detemple-Laake and Eckelmann¹⁰. The nozzle diameter of this tunnel is 180 mm. A circular cylinder of diameter $d=1.5$ mm was mounted horizontally at the nozzle exit. A hot-wire probe was placed in the wake of the cylinder at various $\tilde{x} = x/d$ locations downstream, $y/d = 1$ to one side and halfway between the suspension points of the cylinder. The Reynolds number was varied in the regular region ($50 \leq Re \leq 150$) of the vortex street. The velocity signal was amplified, sampled at 10 kHz and digitalized by a 12 bit A/D converter. Two loudspeakers working 180° out of phase were placed directly above and below the circular cylinder outside the flow to superpose sound. It should be noted that this loudspeaker arrangement is different from that used by Detemple-Laake and Eckelmann⁹.

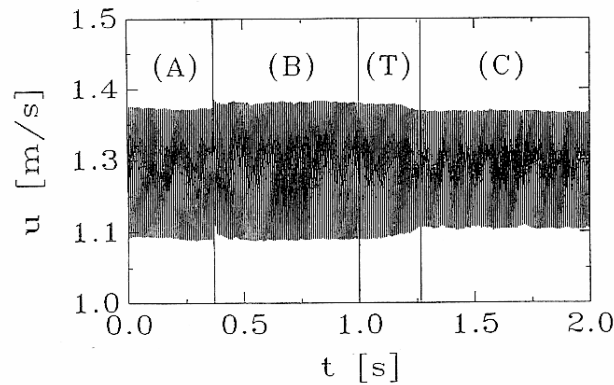


Fig.1. Time series from a Kármán vortex street at $Re = 114$. (A): Vortex street superposed with sound; (B):intermediate region after cutting off the sound; (T): transient state of the vortex street; (C): natural vortex street.

4. A MODEL FOR A KARMAN VORTEX STREET

A typical experimental time series showing the transient behaviour from the stimulated to the natural state of the vortex street is depicted in Fig.1. Four different parts, which can be attributed to different physical processes, are marked. The power spectra for three of these parts are shown in Fig.2. Part (A) in Fig.1 represents the vortex street with parallel vortex shedding stimulated by sound at the sound frequency of $f_s = 119.6\text{Hz}$.

In order to increase the velocity fluctuation amplitude the sound frequency was chosen slightly higher than the natural Strouhal frequency of $f_{st} = 119.0\text{Hz}$. This method of increasing the velocity fluctuation amplitude by stimulating the vortex street with

a slightly different frequency to obtain the transient behavior was developed by the authors. Part (B) in Fig.1 defines the intermediate region between switching off the sound and the beginning of the transient state. Note that in this region, right after switching off the sound, the shedding frequency jumps from f to $f_{max} = 124.5 \text{ Hz}$ (Fig.2 dashed line). Without sound excitation, the unforced parallel shedding of part (B) has a slightly higher frequency than the slantwise shedding of part (C), which is consistent with recent experiments (Ohle et al.¹¹). The last part (C) in Fig. 1 represents the state of the natural vortex street with Strouhal frequency f_{st} and oblique vortex shedding. For the construction of differential equations, which are of the form

$$\begin{aligned} \frac{du_1}{dt} &= u_2; \\ \frac{du_2}{dt} &= \sum_{i,j=0}^{i+j \leq 3} a_{ij}(\tilde{x}) u_1^i u_2^j \end{aligned} \quad (1)$$

only the parts (T) and (C) of the time series were used. In this equation $u_1(t)$ defines the velocity fluctuation amplitude of the Kármán vortex street. Roesch, Eckelmann & Hübler⁸ could verify that in the phase space representation the limit cycles of both the experimental and the simulated data are in good agreement.

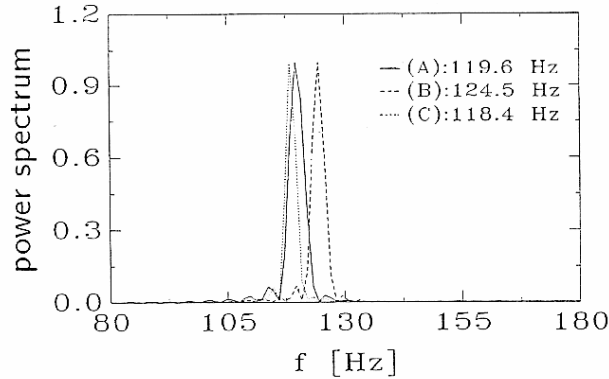


Fig.2. Power spectrum of the parts (A), (B) and (C) of the time series shown in Fig.1.

This guarantees that the dynamics of the vortex street is well represented by the constructed differential equation. The dependence of the normalized coefficients:

$$\alpha_{ij} = \frac{[a_{ij}(\tilde{x}) - a_{ij}(4.7)]}{a_{ij}(4.7)},$$

on the distance \tilde{x} from the cylinder is shown in Fig.3. Since the values of the various

coefficients α_{ij} approach zero for $\tilde{x} \geq 2.5$, it can be concluded that the dynamics of the Kármán vortex street is developed beyond these locations¹⁰. The normalized coefficients

$$\beta_{ij} = \frac{[\alpha_{ij}(Re) - \alpha_{ij}(Re = 53)]}{\alpha_{ij}(Re = 53)}$$

in Fig.4a/b are nearly independent of the Reynolds number for the whole region $50 \leq Re \leq 150$. Special peculiarities like the Tritton¹¹ discontinuity at $Re = 87$, as well as the changes in the shedding modes, described by König, Eisenlohr & Eckelmann¹², are also reflected in the coefficients¹³.

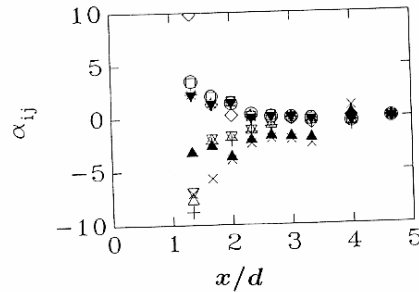


Fig.3. Normalized coefficients α_{ij} as a function of the nondimensional probe distance x/d from the cylinder. Here \square : α_{00} ; $+$: α_{01} ; \times : α_{02} ; \diamond : α_{03} ; \circ : α_{10} ; \triangle : α_{11} ; \blacktriangle : α_{12} ; $*$: α_{20} ; ∇ : α_{21} ; \blacktriangledown : α_{30} .

5. CONTROL OF A KARMAN VORTEX STREET

If it is possible to model the dynamics of an experimental system by differential equations, then it is also possible to predict its dynamics and its response. The basis for a resonant stimulation and specific control of a Kármán vortex street is the extensive knowledge of the differential equations at different Reynolds numbers in the complete wake of the cylinder. The response of such nonlinear oscillators to aperiodic driving forces can be essentially larger than the response to sinusoidal ones. Wagner et al.¹⁴ succeeded experimentally in a resonant stimulation of nonlinear mechanical oscillators with aperiodic driving forces.

With the help of the constructed low-dimensional differential equation control of the Kármán vortex street is also possible. A problem, however, is that a complex system like the vortex street generally has an infinite number of degrees of freedom, whereas

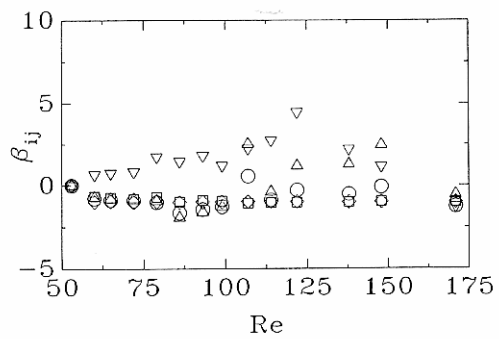


Fig.4a. Normalized coefficients β_{ij} as a function of the Reynolds number. Here Δ : β_{00} ; ∇ : β_{01} ; \square : β_{02} ; \diamond : β_{03} ; \circ : β_{10} .

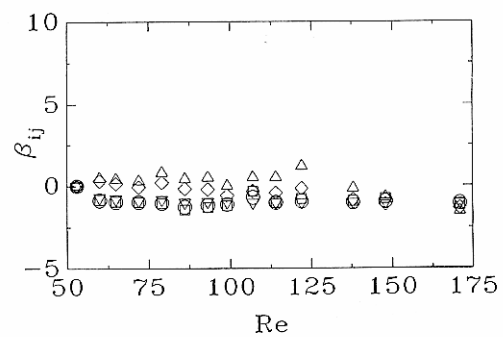


Fig.4b. Same as in Fig.4a. Here Δ : β_{11} ; ∇ : β_{12} ; \square : β_{20} ; \diamond : β_{21} ; \circ : β_{30} .

the constructed differential equation has only two. In spite of this difficulty it is possible to control a complex system such as a Kármán vortex street. It will be now explained by means of the Haken-Wunderlin-Zwanzig equation

$$\begin{aligned}\dot{u} &= \epsilon u - su; \epsilon \ll 1 \\ \dot{s} &= s + u^2\end{aligned}$$

what kind of assumptions a driving force has to satisfy in order to obtain a large and predictable response of the complex system. In this equation the unslaved and slaved modes are denoted as u and s respectively. Since $\epsilon \ll 1$ the unslaved modes u represent a very slowly and nearly constant motion. Therefore the slaved modes s relax very quickly to u^2 , and the Haken-Wunderlin-Zwanzig equation can be reduced to a first order differential equation of the following form:

$$\dot{u} = \epsilon u - u^3.$$

This equation corresponds to our constructed differential equation. By adding a driving force $F(t)$ the equation

$$\dot{u} = \epsilon u - u^3 + F(t) \quad (2)$$

is obtained.

If in contrast the driving force $F(t)$ is added to the original Haken-Wunderlin-Zwanzig equation

$$\begin{aligned}\dot{u} &= \epsilon u - su + F(t); \epsilon \ll 1 \\ \dot{s} &= s + u^2 + F(t)\end{aligned}$$

the unslaved modes u and the driving force $F(t)$ are very slow and nearly constant. Now the slaved modes s relax very quickly to $u^2 + F(t)$ and the equation can be reduced to

$$\dot{u} = (\epsilon - F(t))u - u^3 + F(t).$$

This equation is identical to Eq.(2) only when $F(t) \ll \epsilon$. Thus the constructed differential equation only predicts the correct response of the complex system for resonant, small and slowly driving forces.

Therefore a Kármán vortex street can only be controlled by small driving forces. If the driving force is too large, the slaved modes will also be stimulated, and hence the system can no longer be described by a low-dimensional differential equation. A typical example for the stimulation of slaved modes by a too large driving force was given by Detemple-Laake and Eckelmann⁹. They could stimulate a netting-pattern structure in the wake of a circular cylinder by superposing sound at $Re = 143$. Such a structure normally exists in the transition range ($150 \leq Re \leq 300$).

The experimental problem in the present investigation is that the constructed differential equation describes the situation of a vortex street with oblique shedding. If sound is superposed on such a vortex street parallel shedding will be obtained. Nevertheless, it is possible to control the vortex street to some extent with the constructed differential equation.

By using the constructed differential equation given by Eq.(1) it was found in a computer experiment, that a decrease in the amplitude of the vortex street can be achieved by a sinusoidal driving force, which is raised in frequency of about 10% per second.

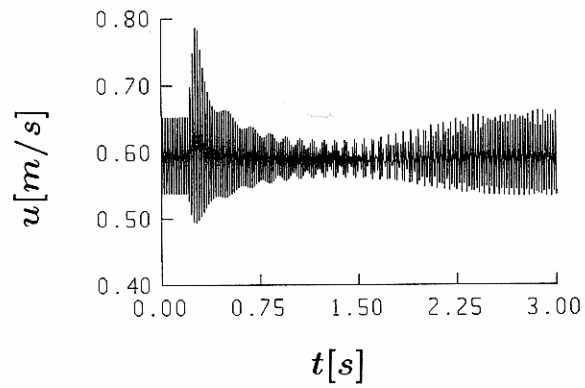


Fig.5: Simulated time series of the constructed differential equation superposed by a sinusoidal driving force with a frequency shift of about 10% per second.

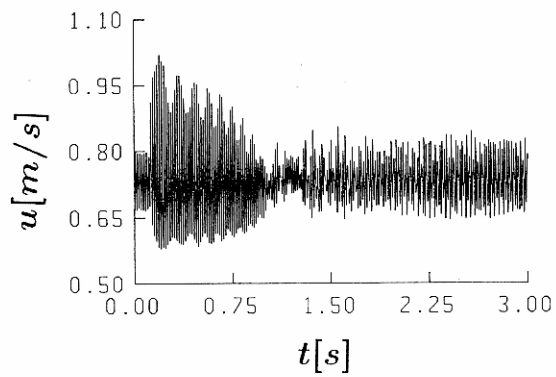


Fig.6: Experimental time series of the Kármán vortex street superposed by the same driving force as in Fig.5.

Fig.5 shows the relevant computer simulation. The typical features of the computer simulation, such as the beat, the decrease in amplitude down to a minimum, and finally the increase back to the natural amplitude can also be found in the experiment (Fig.6). Both, for the experiment, as well as for the computer simulation, the same kind of driving force was used. It should be noted, that the constructed differential equation describing oblique shedding leads to the same behaviour as for the experimental case, where under control conditions parallel shedding exists.

The results presented here can be considered as a first step of an attempt to control a Kármán vortex street without any feedback. For a resonant stimulation the case of parallel shedding should also be incorporated in the construction of the differential equation. Further work along these lines is in progress.

REFERENCES

- 1 Lorenz, E.N., J. Atmospheric Sci. 20, (1963), 130 +448
- 2 Ruelle, D. & Takens, F., Commun. Math. Phys., 20, (1971), 167
- 3 Landau, L.D., C.R. Acad. Sci. URSS, 44, (1944), 311
- 4 Brandstätter, A., Swift, J., Swinney, H.L., Wolf, A., Farmer, J.D., Jen, E. & Crutchfield, P.J., Phys. Rev. Letters 51, (1983), 1442
- 5 Olinger, D.J. and Sreenivasan, K.R., Phys. Rev. Let. 60, (1988), 797
- 6 Benaroya, H. and Lepore, J.A., J.S.V. 86(2), (1983), 159
- 7 Detemple, E., Diplomarbeit Göttingen (1983)
- 8 Roesch, E., Eckelmann, H. & Hübler, A., Max Planck Institut für Strömungsforschung, Göttingen, Report No. 11/1988, (1988)
- 9 Detemple-Laake, E. & Eckelmann, H., Exp. Fluids 7,(1989), 217
- 10 Ohle, F., Lehmann, P., Roesch, E., Eckelmann, H. & Hübler, A., Phys. Fluids A, 4, (1990), 479
- 11 Tritton, D.J., J. Fluid Mech., 6, (1959), 547
- 12 König, M., Eisenlohr, H. & Eckelmann, H., to appear at Phys. Fluids A, 9, (1990)
- 13 Ohle, F., Max-Planck-Institut für Strömungsforschung, Göttingen, Report No. 110/1990, (1990)
- 14 Wagner, C., Stelzel, W., Hübler, A., Lüscher, E. & Altmann, W., Helv. Phys. Acta 61, (1987), 224